Available online at www.sciencedirect.com
SCIENCE DIRECT
Polymer 46 (2005) 6786–6796
polymer
www.elsevier.com/locate/polymer

Simultaneous novel synthesis of conducting and non-conducting halogenated polymers by electroinitiation of (2,4,6-trichloro- or 2,6-dichlorophenolato)Ni(II) complexes

Ş. Özalp-Yaman[a,*], M. Baştürkmen[a], D. Kısakürek[b]

[a]*Chemistry Group, Faculty of Engineering, Atilim University, 06836 İncek Ankara, Turkey*
[b]*Department of Chemistry, Middle East Technical University, 06531 Ankara, Turkey*

Received 18 March 2003; received in revised form 31 May 2005; accepted 1 June 2005
Available online 1 July 2005

Abstract

$NiL_2(Ph)_2 \cdot xH_2O$ [L = 3,5-dimethylpyrazole or *N*-methyl imidazole; Ph = DCP or TCP; $x = 0$, 1 or 3] complexes were synthesised and characterised by analytical and spectroscopic methods using elemental analysis and FTIR. The electrochemical behavior of the complexes was studied by cyclic voltammetry in tetrabutylammoniumtetrafluoroborate–*N*,*N*-dimethylformamide electrolyte–solvent couple. Cyclic voltammogram of the complexes displayed two-step oxidation processes under the nitrogen gas atmosphere. The polymerization of the complexes was accomplished in the same solvent–electrolyte couple by the constant potential electrolysis of $NiL_2(Ph)_2 \cdot xH_2O$, synthesizing the poly(di- or monochlorophenylene oxide)s via free radical mechanism. The simultaneous polymerization of non-conducting polymer and conducting polymer (the conductivity of 0.7 S cm^{-2}) were achieved by electroinitiated polymerization of $Ni(DMPz)_2(TCP)_2$. The structural analysis of the polymers were performed using FTIR, ^1H NMR and ^{13}C NMR spectroscopic techniques and DSC for the thermal analysis. The kinetics of the polymerization was followed by in situ UV–vis spectrophotometer during the electrolysis. The low temperature ESR spectrum of the electrolysis solution also confirmed the formation of phenol radical ($g = 2.0028$). One electron oxidation process of $NiL_2(DCP)_2 \cdot xH_2O$ produces a new Ni(II) complex, Ni(L–L)$(DCP)_2$(S) by the rapid decomposition of $Ni^{III}L_2(DCP)_2$ into a ligand radical producing a singlet with the *g* value of 2.0015. Second electron oxidation process generates oligemers, which could not be isolated from the electrolyte solution.

Keywords: Poly(di- and monochlorophenylene oxide); Conducting polymer; Electroinitiated polymerization

1. Introduction

The original electrolysis of silver of 2,4,6-trihalogenated phenol in pyridine was achieved at the anode, having an amorphous polymer, poly(dihalophenylene oxide) [1]. Later, there were various reports of electroinitiated polymerization of phenols and its derivatives [2–6] and various 2,4,6-trihalophenolato Cu(II) [7–19] and Ni(II) [20] complexes with mainly pyridine and to some extent ethylenediamine and *N*,*N*,*N*′,*N*′-tetramethylethylenediamine substituted as chelating and non-chelating ligands. No accounts appear on the electroinitiated polymerization of Ni complexes of tri- and di-substituted chlorophenols in the presence of dimethylpyrazole and *N*-methylimidizole neutral ligands.

There have been numerous attempts to prepare novel synthesis of conducting polymers by electrochemistry. Several studies have been carried out in the presence of conducting polymers, on the preparation of organic transistors [21,22], light-emitting diodes [23,24], biosensors [25,26], modified electrodes [27,28] and electrochromic devices [29–34]. Also, very recently, the simultaneous polymerization of conducting and non-conducting polymers were achieved by microwave initiation of sodium 2,4,6-trichlorophenolate [35].

It is well known that too laborious synthetic approach would not be practical for industrial applications. Hence, in the present work, new bis(2,4,6-tri- and 2,6-dichlorophenolato)bis(3,5-dimethylpyrozole)Ni(II) and bis(2,4,6-tri- and 2,6-dichlorophenolato)bis(*N*-methlimidizole)Ni(II)

* Corresponding author. Fax: +90 586 80 91.
E-mail address: seniz@atilim.edu.tr (S¸ Özalp-Yaman).

0032-3861/$ - see front matter © 2005 Elsevier Ltd. All rights reserved.
doi:10.1016/j.polymer.2005.06.005

complexes were synthesized and used for simultaneous synthesis of conducting and non-conducting polymers by electroinitiation.

2. Experimental

2.1. Materials

N-Methyl imidazole (*N*MIz), 2,6-dichlorophenol (DCP) and 2,4,6-trichlorophenol (TCP) were provided by Aldrich (99%) and were used without further purification. 3,5-Dimethyl pyrazole (DMPz) and $NiSO_4 \cdot 6H_2O$ were purchased from Merck (99%) and NaOH were provided by Fluka (98%). Tetrabutylammoniumtetrafluoroborate, (TBATFB) used as an electrolyte for cyclic voltammetry measurements was provided by Merck Co. *N*,*N*-Dimethylformamide (DMF) (Riedel 99%) was commercially available reagent grade and was used as received.

2.2. Preparation of nickel complexes

$Ni(DMPz)_2(DCP)_2 \cdot H_2O$ (**C1**), $Ni(DMPz)_2(TCP)_2$ (**C2**), $Ni(NMIz)_2(DCP)_2 \cdot 3H_2O$ (**C3**) and $Ni(NMIz)_2(TCP)_2 \cdot 3H_2O$ (**C4**) were prepared from the aqueous solutions as reported in literature for the other analogues [36,37]. 6.21 mmol TCPH (or DCPH), NaOH and *N*-methylimidazole (or 3,5-dimethylpyrazole) were dissolved in 50 cm^3 distilled water added into the 50 cm^3 aqueous 3.21 mmol $NiSO_4 \cdot 6H_2O$ solution drop wise with stirring. The precipitated complex filtered, washed with distilled water and dried to a constant weight under vacuum.

2.3. Characterization of the complexes

2.3.1. Elemental analysis

Carbon–hydrogen–nitrogen analysis of complexes was carried out by Leco 932 CHNSO elemental analyzer. Elemental analysis results indicate the presence of crystalline water in some of the complexes. Elemental analysis results of the complexes (**C1–C4**) (experimental errors $\pm$ 0.5) are:

Compounds	%C		%H		%N	
	Calc.	Found	Calc.	Found	Calc.	Found
C1	44.56	44.89	4.08	3.95	9.45	9.40
C2	41.04	41.07	3.13	2.99	8.70	8.57
C3	39.97	40.00	4.25	4.41	9.32	9.21
C4	35.86	35.94	3.31	3.19	8.36	8.35

2.3.2. Fourier-transform infrared analysis

FTIR spectra of the complexes were recorded on a Nicolet 510 FTIR spectrometer dispersed in KBr discs and for spectroelectrochemical studies a HP 8453 A diode array UV–vis spectrophotometer was used with a specially designed cell which allows monitoring spectral changes during the potential applications. The FTIR spectrum of **C1–C4** exhibited characteristic C–O stretching at 1238–1271, C–N stretching in the range of 1450–1582 and O–H stretching at 3500 cm^{-1} due to the presence of crystalline water. Electronic absorption band maxima of **C1–C4** and the corresponding molar extinction coefficients, ε, in DMF were presented in Table 1.

2.4. Electrochemistry

Electrochemical behavior of the complexes was investigated by cyclic voltammetry (CV) by using Volta Lab PGZ 301 Dynamic Voltammeter in DMF–TBATFB solvent–electrolyte couple versus saturated calomel reference electrode (SCE) under nitrogen gas atmosphere at room temperature. A platinum bead working and a platinum coil counter electrodes were used for CV measurements. The concentrations of the complexes were 0.001 M for each measurement and voltage scan rate during the CV measurements was 200 mV/s.

Constant potential electrolysis at the peak potentials was carried out in DMF vs Ag-wire reference electrode after making the correction between SCE and the Ag wire (the oxidation potential of ferrocene/ferrocenium couple was found to be 0.84 V vs SCE and 0.56 V vs Ag-wire in our system). Platinum plate (1.5 cm^2) electrodes served as a working and counter electrode as well. The oxidation process was followed in situ by UV–vis spectrophotometer during the electrolysis. Platinum gauze electrodes were used as working and counter electrode vs Ag-wire during the spectroelectrochemical studies. Electronic absorption spectra were recorded for every 50 mC and nitrogen gas was bubbled through the electrolysis solution for stirring purposes between the scans.

2.5. Polymer synthesis

Electrochemical polymerization of the complexes (**C1–C4**) were achieved by using constant potential electrolysis for 6 h at 100 mV more positive potentials than their second peak potentials vs Ag-wire under nitrogen gas atmosphere at room temperature by using Volta Lab PGZ 301 Dynamic Voltammetry. 0.02 M complex solution in 20 cm^3 DMF was used during the electrolyses. At the end of the electrolysis, anolyte was poured in to 150 cm^3 ethanol containing few drops of concentrated HCl to precipitate the polymer. Polymers were collected by vacuum filtration and dried under vacuum until constant weight at room temperature.

2.6. Polymer characterization

2.6.1. Electron spin resonance

The ESR spectrums of the electrochemically generated products were recorded by Bruker Xepr ELEXSYS-580

Table 1
Electronic absorption spectral data for **C1–C4** in DMF

Compound	Electronic spectra λ_{max} (nm) (log ε (cm^{-1} mol^{-1} L))
C1	267(3.83), 279(3.81), 286(3.78), 315[a](3.43), 324[a](3.45), 333(3.47), 380[a](2.31), 454(1.87), 553[a](1.49), 801(1.38)
C2	268(4.16), 288[a](3.78), 297[a](3.76), 324[a](3.77), 3.87[a](2.12), 343(3.88), 440[a](1.65), 543(1.23), 774(1.20)
C3	268(3.71), 279(3.74), 286(3.72), 312(3.40), 336(3.34), 407[a](1.97), 465[a](1.64), 724(1.40), 762[a](1.36), 796(1.36)
C4	269(4.12), 297(3.64), 344(3.82), 339[a](3.81), 396[a](2.07), 702(1.28)

[a] Shoulder.

spectrometer in quartz EPR cell in liquid nitrogen where diphenylpicrylhydrazyl (DPPH) was used as a reference.

2.6.2. Fourier-transform infrared analysis

FTIR spectra of the polymers were recorded on a Nicolet 510 FTIR spectrometer with polymers dispersed in KBr discs.

2.6.3. Nuclear magnetic resonance analysis

^{1}H NMR and decoupled ^{13}C NMR spectra of polymers were recorded on a Bruker GmbH DPX-400, 400-MHz high-performance digital FT NMR, using $CDCl_3$ as a solvent and TMS as an internal reference.

2.6.4. UV–vis analysis

HP 8453 A diode array UV–vis spectrophotometer was used for polymer characterizations.

2.6.5. Differential thermal analysis

Thermal behavior and the glass transition temperatures of the polymers were carried by a DuPont thermal analyst 2000 DSC 910S model differential scanning calorimeter under nitrogen atmosphere. The scanning rate was 10 °C/min for 6–10 mg polymer samples.

2.6.6. Scanning electron microscope analysis

Analysis of the surface morphologies of films were done by using JEOL JSM-6400 scanning electron microscope having photo edit attachment Noran instrument EDS X-ray microanalysis system.

2.6.7. Conductivity measurements

Conductivity of the black product on the electrode surface was determined by four-probe technique (0.7 S cm^{-2}).

3. Results and discussion

3.1. Voltammetric studies

The electrochemical data for all complexes are presented in Table 2. Voltammograms of all Ni(II) complexes exhibit two irreversible oxidation processes in DMF at room temperature under nitrogen gas atmosphere. As the scan direction reversed, a cathodic peak depending on the second oxidation peak was observed between −0.48 and −0.64 V vs SCE (Fig. 1).

A linear dependence, which was observed between I_p and $V^{1/2}$ and between E_p and I_p as the voltage scans rate (V) increased, reveals the diffusion controlled electron exchange reaction. According to the Nicholson–Shain criteria [38] the negative slop of the plot of $I/CV^{1/2}$ versus log V indicates a reversible electron exchange followed by a chemical reaction. However, appearance of irreversible peaks in the cyclic voltammogram can be explained by a higher rate of chemical reaction following the electrochemical one in DMF.

3.2. Electrochemical polymerization

Electrochemical oxidation of the Ni(II) complexes (**C1–C4**) was carried out 100 mV more positive potentials than their second peak potentials in DMF–TBATFB solvent–electrolyte couple vs Ag-wire, for 6 h. However, polymers were only isolated from the anolyte solution of **C2** and **C4** by the addition of slightly acidic ethanol solutions. The yields were calculated as 40–44% for the polymers by regarding the metal and ligands incorporation into the polymer [36,37].

The FTIR spectrum of **P2** (the polymer obtained by the electrooxidation of **C2**) is presented in Fig. 2. The

Table 2
Cyclic voltammetry data (VSR = 100 mV/s) for **C1–C4** in DMF

Compound	In DMF		In acetonitrile	
	E_a (V)	E_c (V)	E_a (V)	E_c (V)
C1	0.48, 1.13	−0.64[a]	0.49, 1.31, 1.62	0.37,[a] −0.60
C2	0.58, 1.20	−0.48[a]	0.60, 1.22	0.48[b]
C3	0.49, 1.17	−0.62[a]	0.53, 1.20	0.26,[a] −0.64
C4	0.54, 1.13	−0.48[a]	0.59, 0.95, 1.40	−0.45,[b] −0.75

E_a represents the oxidation peak potential. E_c represents the reduction peak potential.
[a] Dependence on the 2nd peak potential.
[b] Dependence on the 1st oxidation peak potential.

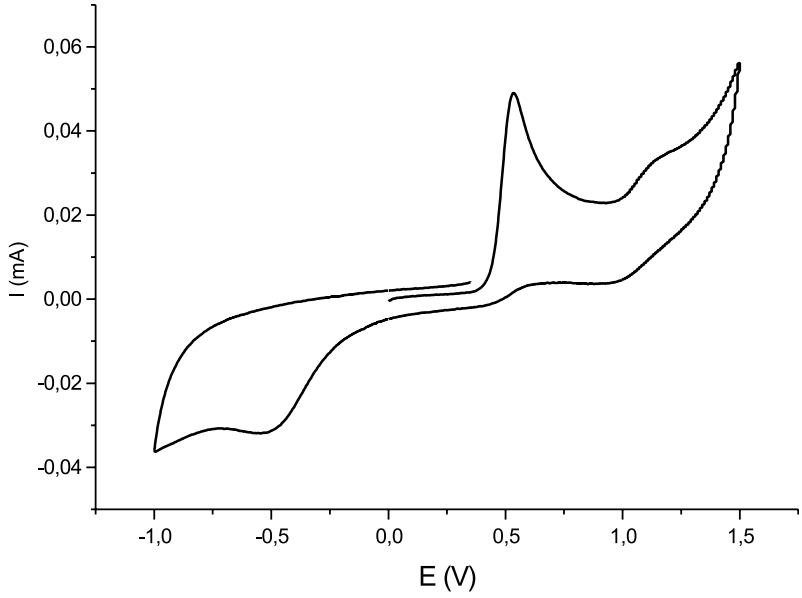

Fig. 1. Cyclic voltammogram of 0.001 M **C2** in DMF at room temperature vs SCE (VSR = 200 mV/s).

absorption bands between 1387 and 1609 cm^{-1} are the C=C ring strechings. The spectrum displays C–O bands (1143–1249 cm^{-1}), C–O–C strechings (943–1086 cm^{-1}), C–H bands (822, 861 cm^{-1}) and C–Cl absorptions (726, 770 cm^{-1}). The broad peak observed at 3335 cm^{-1} was attributed to the phenolic end groups.

Poly(dichlorophenylene oxide) was characterized by ^{13}C-decoupled and ^{1}H NMR spectrometer in deuterated chloroform. ^{13}C-decoupled spectrum of **P2** is shown in Fig. 3. For the theoretically calculated ^{13}C NMR chemical shift data correlation tables [39] were used to examine the spectrum for the three main possible addition products: 1,2; 1,4; both 1,2 and 1,4 adducts [37]. A close inspection of the Fig. 3 clearly indicates the both 1,2 and 1,4 additions were possible. The ^{1}H NMR spectrum of **P2** (Fig. 4) revealed that the peak at δ 7.3–7.4 ppm due to the protons of 2,6 dichloro-1,4-phenylene oxide units (1,4 addition); and the peak at δ 8.0 ppm were due to 2,4-dichloro-1,6-phenylene oxide units (1,2 addition). Thus it can be clearly observed that 1,2- and 1,4- additions are taking place at equal rates. The higher

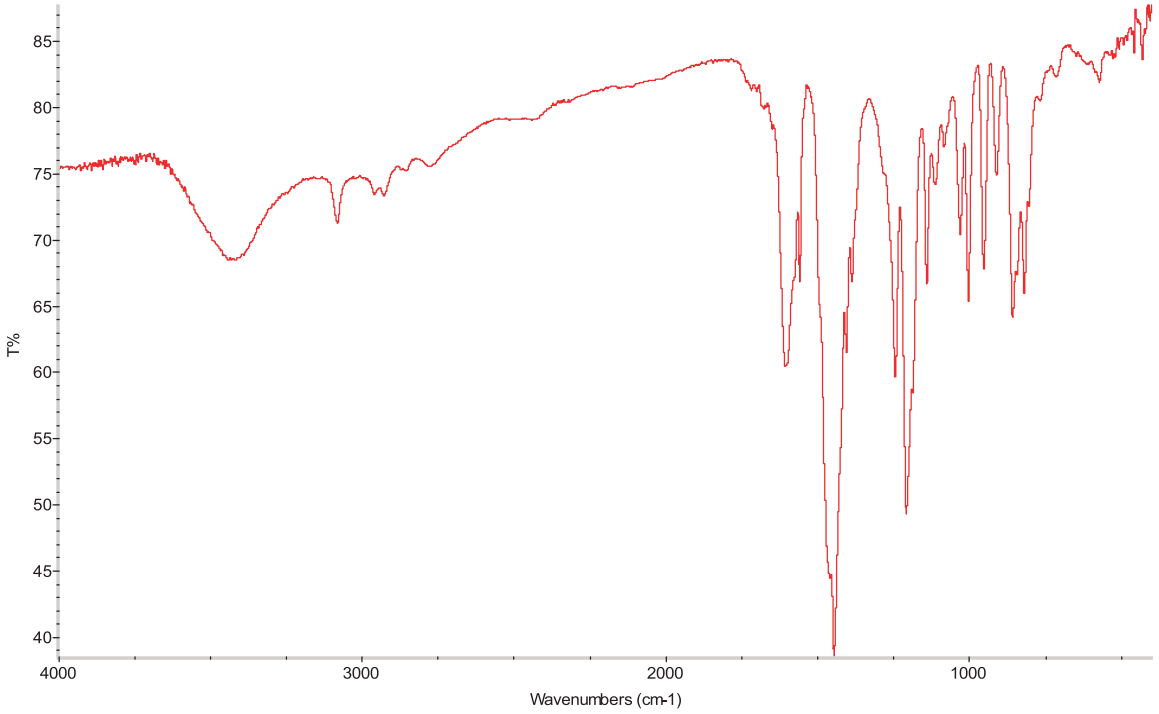

Fig. 2. FTIR spectrum of **P2**.

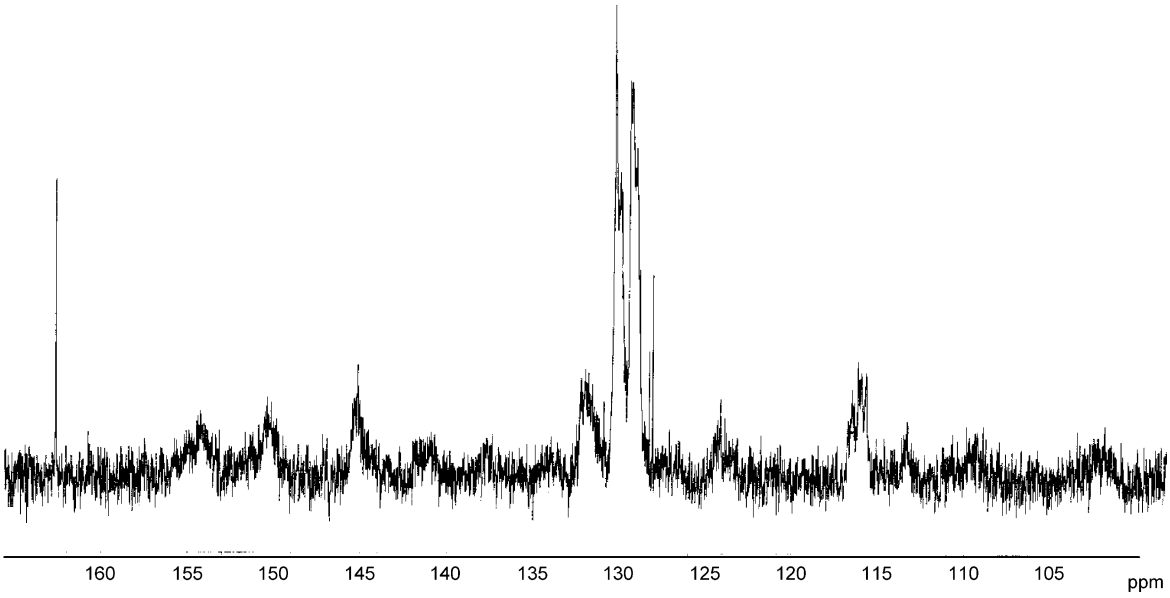

Fig. 3. Proton decoupled ^{13}C NMR spectrum of **P2**.

field broad lines can be assigned to branched units of both 1, 2- and 1,4- additions on the same monomeric unit [37]. Thermal behavior of poly(dichlorophenylene oxide) was studied by differential scanning calorimeter. The glass transition temperature of polymer was 159.5 °C indicating high rigidity.

The surface of the counter electrode was coated with a thin black polymer film indicating the possibility of formation of a conducting polymer (**CP2**) during the anodic oxidation of **C2**. The electrochemical reduction of **C2** was attempted at 100 mV more negative potential than its reduction peak in DMF vs Ag-wire for 6 h, as well. An extremely thin layer of a black conducting polymer with a conductivity of 0.7 S cm^{-2} was observed on the surface of the electrode; however, the amount was not sufficient enough to make any further analysis other than the conductance measurement and the surface morphology analyses.

Analysis of the surface morphologies of the conducting polymer was done by scanning electron microscope,

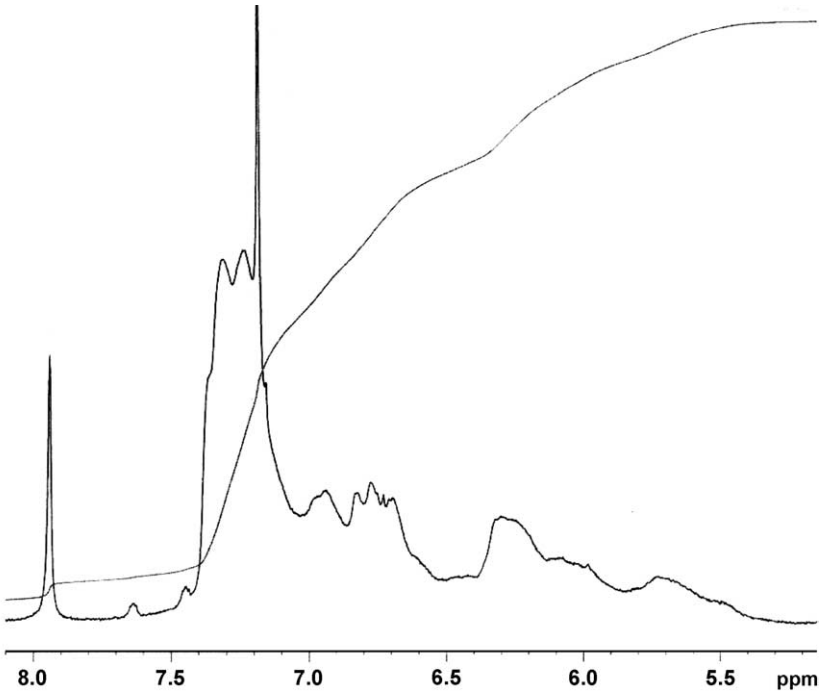

Fig. 4. ^{1}H NMR spectrum of **P2**.

(Fig. 5(a–d)). In Fig. 5(a), black strips were observed due to non-conducting polymer when magnified by 20. However, in Fig. 5(a), black strips were observed due to non-conducting polymer when magnified by 20. When this area was magnified by 2000, growing of a standard cauliflower-like structure conducting polymer through the non-conducting surface was clearly be observed (Fig. 5(b)). Fig. 5(c), showed the distribution of the cauliflower-like structure only on the conducting polymer surfaces. In Fig. 5(d), the clear appearance of the cauliflower-like structure was seen when (b) magnified 20,000 times. The X-ray microanalysis system detected the existence of Ni, Cl and C on both black and white areas whereas detected F on the black strip and O in white side.

3.3. Spectroelectrochemical oxidation

Spectral analysis of the polymers **P2** and **P4** (the polymer obtained by the electrooxidation of **C4**) was also carried out by UV–vis spectrophotometer. Both polymers were found to be structurally identical. Electronic absorption spectrum of **P2** and **P4** exhibit exactly the same absorption band at 279 nm, which could be assigned as the $\pi \rightarrow \pi^*$ transitions of the aromatic ring and two shoulders at 269 and 284 nm (Fig. 6).

All these spectral observations are consistent with the following electrode reaction mechanism given in Eqs. (1)–(3).

$$NiL_2(TCP)_2 \rightarrow NiL_2(TCP)(X) + TCP\bullet + 1e^- \quad (1)$$

$$TCP\bullet + NiL_2(TCP)_2 \rightarrow NiL_2(DCP\text{–}TCP)X \quad (2)$$

$$\rightarrow \rightarrow \rightarrow \rightarrow \quad \text{Poly(DCP)} + NiL_2(X)_2 \quad (3)$$

where X is chlorine, TCP is 2,4,6-trichlorophenolate, DCP is dichlorophenolate and L is 3,5-dimethylpyrazol or *N*-methyl imidazole. As described in the Eqs. (1)–(3), the polymerization proceeds via free radical mechanism upon

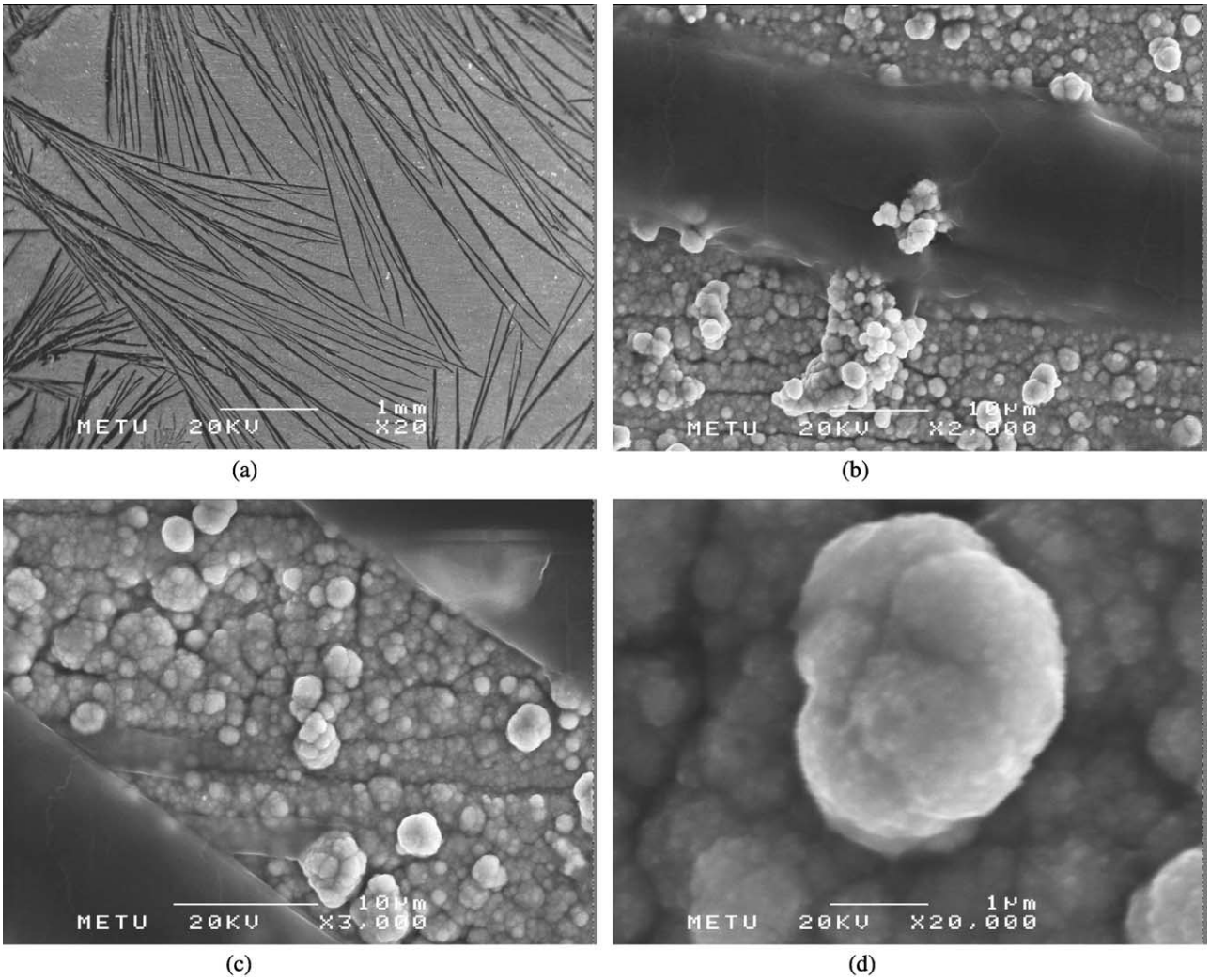

Fig. 5. SEM micrographs of **CP2** magnified by (a) ×20, (b) ×2000, (c) ×3000 and (d) ×20,000.

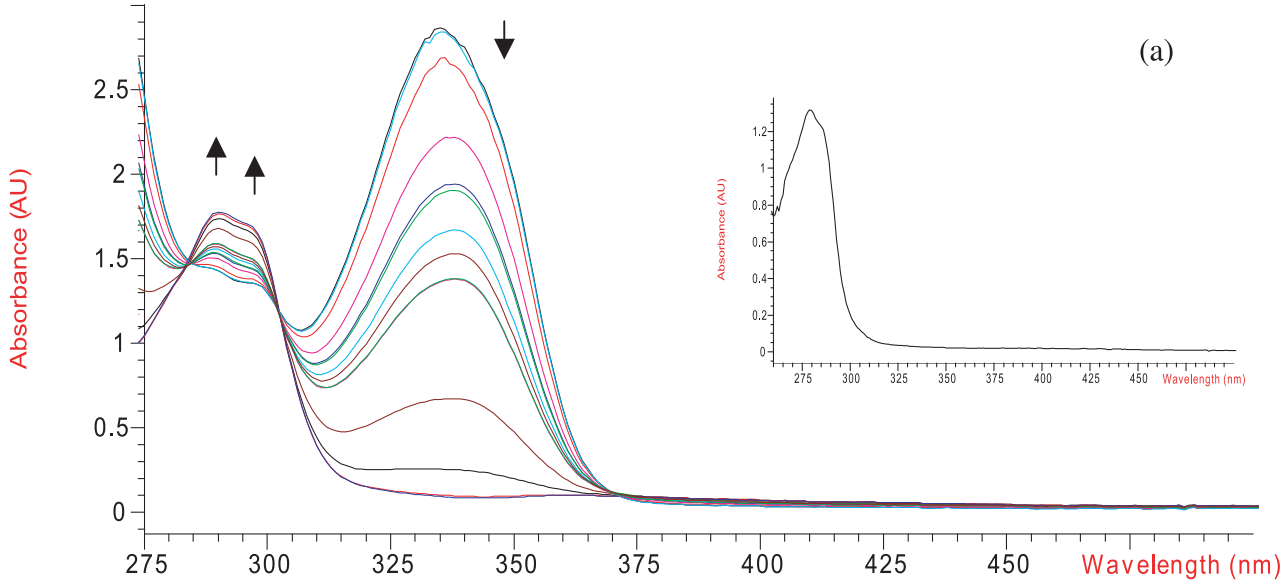

Fig. 6. The changes in the electronic absorption spectrum of 3.80×10^{-4} M **C2**. (Inset: The electronic absorption spectrum of **P2** in DMF).

the oxidation by producing poly(dichlorophenylene oxide) [7,10,17].

The electrochemical oxidation of the complexes (**C1**–**C4**) were investigated in situ by recording the spectral changes, are shown in Figs. 6 and 8. During the one electron oxidation, the intensity of the characteristic band of **C2** at 335 nm decreased while two new bands formed at 289 and 297 nm with three well defined isosbestic points at 285, 302 and 370 nm. Decline in the intensity of the band at 335 nm continued during the second electron transfer (Fig. 6) and disappeared completely at the end of the electrolysis, while the intensity of the bands at 289 and 297(sh) nm increased, implying the formation of poly(dichlorophenylene oxide) in the electrolyte solution. The similar spectral changes were observed during the electrochemical oxidation of **C4**, monitored in situ by UV–vis spectrophotometer.

The ESR spectrum of the electrochemically generated product was taken after the first and the second electron

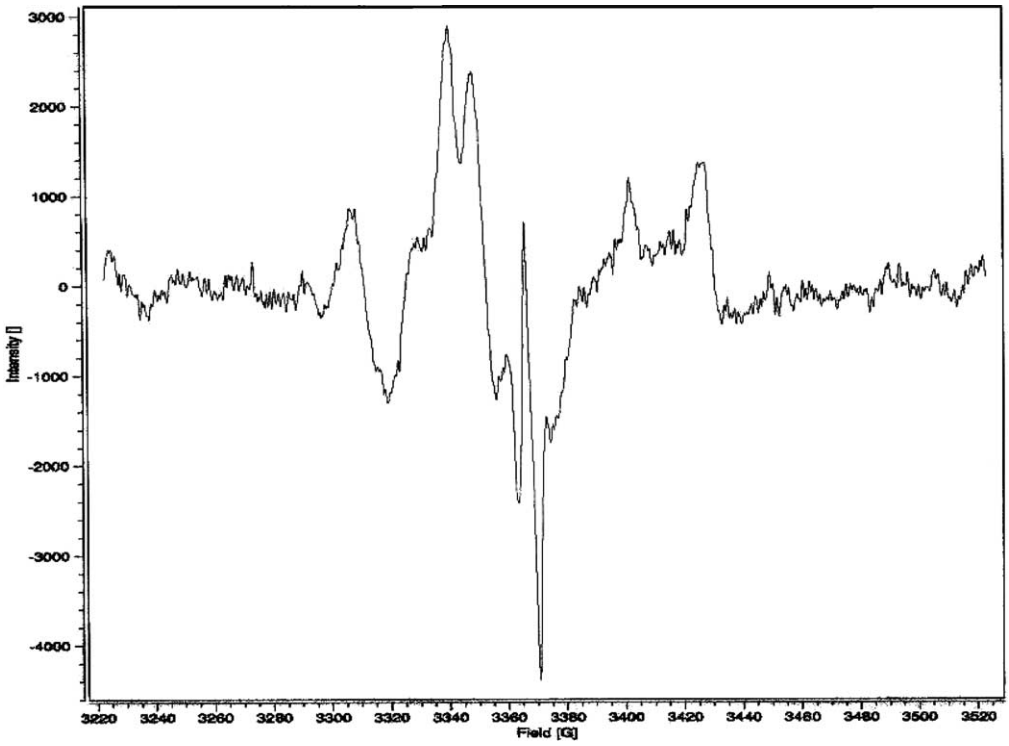

Fig. 7. EPR spectrum of phenoxy radical at 150 K.

transfer revealed the same signal with the *g* value of 2.0028, which was very close to the g value of free electron. Superhyperfine splittings could be assigned due to the neighbouring H-atoms in the molecular structure (Fig. 7). This singlet must be due to the formation of phenoxy radical, leading to a free radical mechanism for the electrochemical polymerization of **C2** and **C4** as described in the Eqs. (1)–(3).

Spectroelectrochemical behaviors of **C1** and **C3** were different compared that of the **C2** and **C4**. A gradual decrease in the intensities of the original bands of **C1** at 323 and 385(sh) nm were observed while new bands formed at 435, 457, 471, 706(sh), 755 and 878 nm during the one electron transfer (Fig. 8(a)). Two isosbestic points which indicate only one step electrode reaction was also obtained at around 294 and 350 nm.

The ESR spectrum of the product (Fig. 9) obtained after the one electron transfer at −10 °C exhibited a singlet

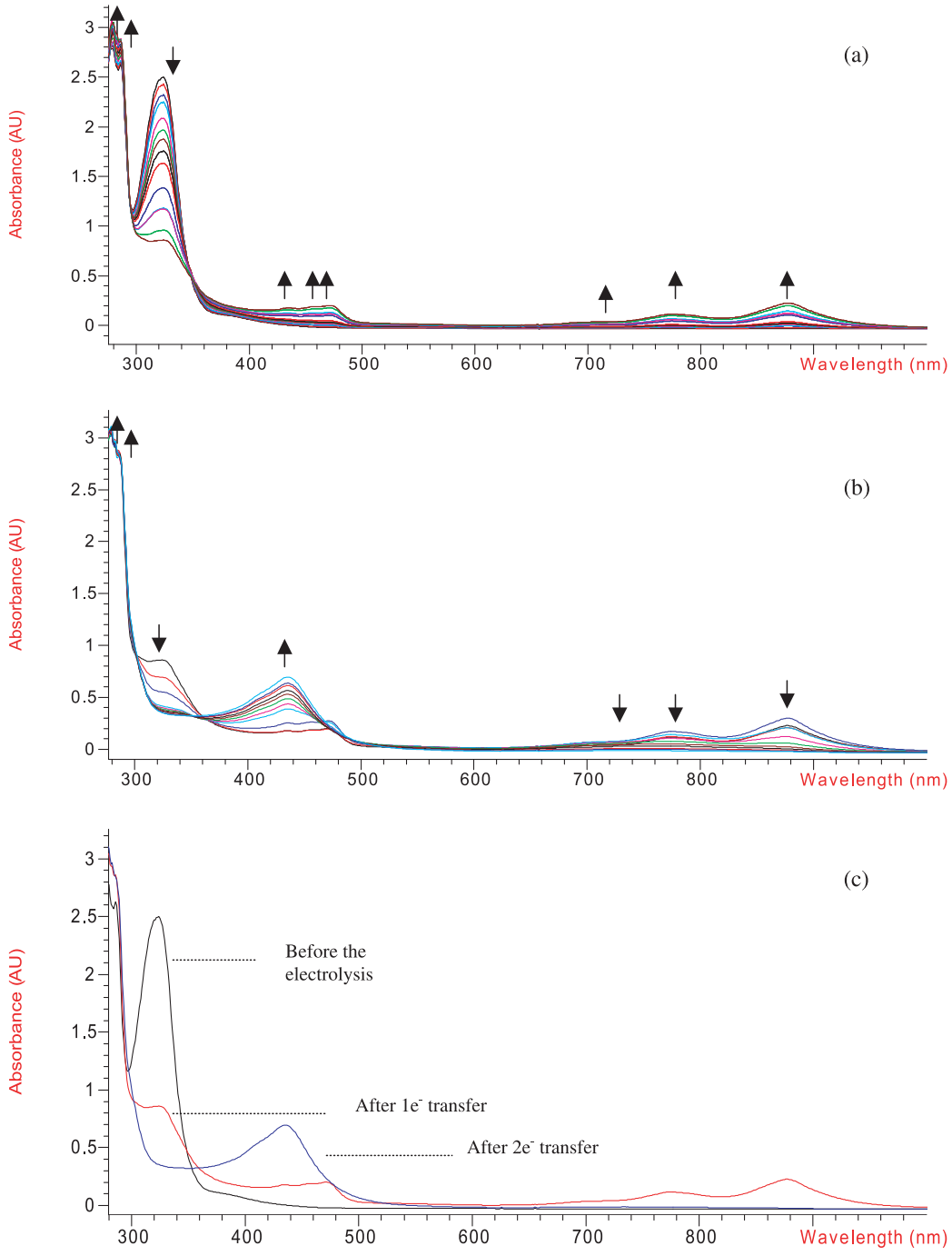

Fig. 8. (a) The changes in the electronic absorption spectrum of 5.23×10^{-4} M **C1** between the two scans; (b) during the second electron transfer; (c) before the oxidation, the one electron transfer and the end of the electrolysis.

($g = 2.0015$) revealing the formation of an organic radical different than the phenoxy radical. Although the formation of new d–d transition bands in the electronic absorption spectrum of **C1** and **C3** indicated the generation of a new Ni(II)-complex in the electrolyte solution, no ESR signal was obtained corresponding to the Ni(III)-species due to its extremely short half life.

Hence, the mechanism of the electrochemical oxidation process of **C1** and **C3** can be proposed by the Eqs. (4) and (5).

$$Ni^{II}L_2(DCP)_2 \rightarrow Ni^{III}L_2(DCP)_2 + 1e^- \quad (4)$$

$$Ni^{III}L_2(DCP)_2 \rightarrow Ni^{II}L(DCP)_2(S) + L\bullet \rightarrow Ni^{II}(L\text{–}L) \times (DCP)_2(S) + H^- \quad (5)$$

where (L–L) is the dimer of the ligands having N–N bridge, DCP is 2,6-dichlorophenolate and S is the solvent molecule. During the oxidative electrolysis, an electron is reversibly removed from the nickel complex, $Ni^{II}L_2(DCP)_2$, forming $Ni^{III}L_2(DCP)_2$, which is not stable at room temperature and immediately dissociates into $Ni^{II}L(DCP)_2(S)$ and the ligand radical, $L^{\cdot}$. At low temperature $L^{\cdot}$ is stable enough to observe an ESR signal with the g value of 2.0015 as presented in the Fig. 9. This radical then reacts with $Ni^{II}L(DCP)_2(S)$ complex by attacking the coordinated L to yield $Ni^{II}(L\text{–}L)(DCP)_2(S)$ and H^- ion as final products. Moreover, the d–d transition bands appeared in the electronic absorption spectrum of **C1** during the one electron oxidation process could be associated with the formation of $Ni^{II}(L\text{–}L)(DCP)_2(S)$.

Further controlled potential electrolysis of the above electrolysed solution was also monitored (Fig. 8(b)) during the second electron transfer at the same peak potential. The original bands of the complex disappeared completely and the bands obtained at 435, 457 and 471 nm combined to form two bands at 435 and 414(sh) nm. On the other hand intensity of the bands appeared at low energy region (706, 755 and 878 nm) decreased and disappeared at the end of the process. During these changes, two new bands appeared at around 279 and 287 nm with a new isosbestic point at 520 nm, clearly implied the presence of poly(chlorophenylene oxide) chain in the electrolyte solution (Fig. 8(c)).

The low temperature ESR spectrum taken after the second electron transfer process proceeded at $-10\,^{\circ}C$, revealed a signal which is strikingly similar to that was obtained during the electrolysis of **C2** and **C4**, leaving no doubt to that phenoxy radical formation at the end of the electrolysis (Fig. 7).

In the light of the above discussion, a possible

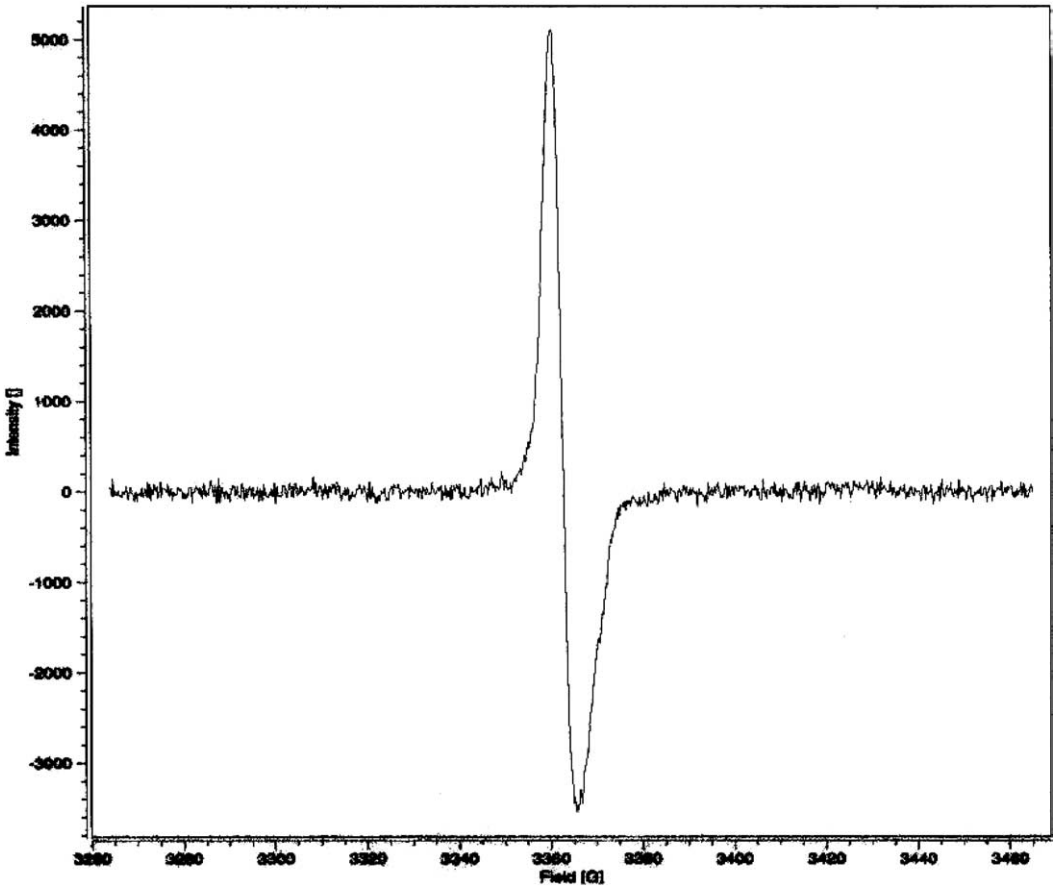

Fig. 9. EPR spectrum of $L^{\cdot}$ produced during the one electron transfer process of **C1** at 150 K.

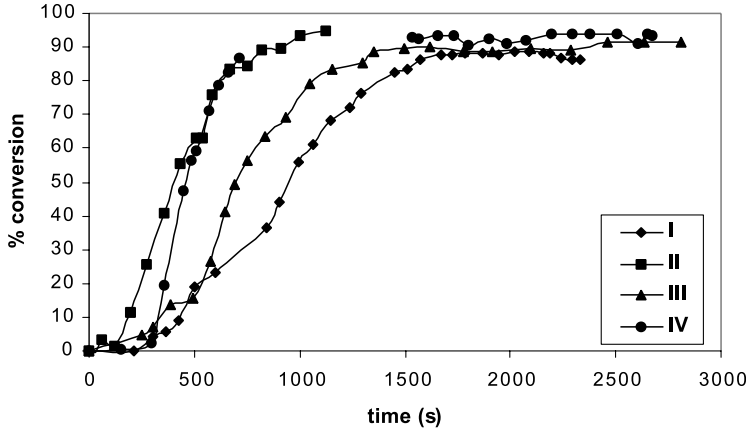

Fig. 10. Percent conversion of complexes **C1**–**C4**.

mechanism for the electrochemical oxidation after the second electron transfer of **C1** and **C3** as follows,

$$Ni^{II}(L\text{–}L)(DCP)_2(S)Ni^{II}(L\text{–}L)(DCP)(S)_2 + DCP\bullet + e^- \quad (6)$$

$$DCP\bullet + Ni^{II}(L\text{–}L)(DCP)_2(S) \rightarrow\rightarrow\rightarrow \text{poly(CP)} + Ni^{II}(L\text{–}L)(X)_2(S) \quad (7)$$

where X, DCP and CP are chlorine, dichlorophenolate and chlorophenylene oxide, respectively.

Since the polymerization process proceeded in the presence of a byproduct (NiL_2X_2) during the oxidative electrolysis of **C1** and **C3**, the molecular weight of the poly(dichlorophenylene oxide)s produced was not high enough to be precipitated. Here the formation of an oligomer should be also taken into account.

The higher tendency of removing an electron from a metal based orbital rather than a monomer based orbital can be related with the higher electron withdrawing ability of the chlorine in the para position. In the complexes **C2** and **C4** the para position of the phenolate is occupied by the chlorine, which attracts the electron density on the metal towards the monomer ring. Hence, electron is transferred from the monomer (phenolate) based orbital rather than the metal based one during the electrochemical oxidation. Contrary to **C2** and **C4**, the para position is empty in the phenolates coordinated to **C1** and **C3**, leading to the higher electron density on the metal center. Therefore, production of the polymer occurs with the formation of a by-product by the oxidation of the metal center before the monomer.

Since, the anodic peaks of the side products, NiL_2X_2 and $Ni(L\text{–}L)X_2(S)$, formed as the polymerisation proceeded, obscured the anodic peak of the unreacted monomer, CV measurements could not be used to determine the percent conversion of monomer. Instead, the spectral changes recorded during the electrochemical oxidation of the complexes **C1** to **C4**, were undertaken to achieve the kinetic study of the polymerisation. The percent conversion increased slowly to 4% at the end of the 200 s induction period and than a sudden increase up to 90% was observed as depicted in Fig. 10.

4. Conclusion

In the present study, the electrochemical behaviour $NiL_2(Ph)_2 \cdot xH_2O$ [L = 3,5-dimethylpyrazole or *N*-methyl imidazole; Ph = DCP or TCP; $x = 0$, 1 or 3] was studied by cyclic voltammetry. The smallest first oxidation peak potentials were obtained when the phenolate is DCP, indicating the rapid decomposition of the complexes compared to that of the complexes containing TCP.

$Ni(L_2)(TCP)_2$ complexes can be polymerised in DMF by electrochemical oxidation in high yields but having low molecular weights (less than 7×10^3) [7–20]. The electrochemical initiation yields 1,2- and 1,4- addition products. Oxidative electrolysis of $Ni(L_2)(DCP)_2$ complexes, however, generates a new Ni(II) complex, $Ni^{II}(L\text{–}L)(DCP)_2(S)$ as a by-product, leading to the lower yield in poly(chlorophenylene oxide).

For the first time, highly conducting ($0.7\ S\ cm^{-2}$) cauliflower-like structure black polymer, having completely different structure than microwave initiated polymerization [35] and non-conducting polymer were synthesized simultaneously from $Ni(TCP)_2$ complex by electroinitiated polymerization technique only when substituted ligand was DMPz. The glass transition temperature of polymer was 159.5 °C indicating high rigidity.

Acknowledgements

Partial financial support by METU and AU research fund is gratefully acknowledged.

References

[1] Hunter WH, Whitney RB. J Am Chem Soc 1932;54(335):1167.
[2] Breitenbach JW, Srna C, Olaj OF. Macromol Chem 1960;42:171.
[3] Akbulut U, Eren S, Toppare LK. J Macromol Sci Chem 1984;A21(3): 335.
[4] Yurttaş B, Toppare L, Akbulut U. J Macromol Sci Chem 1988;A25: 219.
[5] Dubois JE, Laceze PC, Pham MC. J Electroanal Chem 1981;117:233.
[6] Yamamuto K, Nishide H, Tsuchide E. Makromol Chem 1987;8:11.
[7] Sacak M, Akbulut U, Kısakürek D, Turker L, Toppare L. J Polym Sci, Part A: Polym Chem 1989;27:1599.
[8] Turker L, Kısakürek D, Sen S, Toppare L, Akbulut U. J Polym Sci, Part B: Polym Phys 1989;26:2485.
[9] Sen S, Kısakürek D, Turker L, Toppare L, Akbulut U. New Polym Mater 1989;1(3):177.
[10] Yiğit S, Kısakürek D, Turker L, Toppare L, Akbulut U. Polymer 1989; 30:348.
[11] Sacak M, Akbulut U, Kısakürek D, Toppare L. Polymer 1988;30:928.
[12] Akbulut U, Sacak M, Kısakürek D, Toppare L. J Macromol Sci Chem 1989;A26(12):1623.
[13] Akbulut U, Sacak M, Kısakürek D, Toppare L. Br Polym J 1973;95: 5707.
[14] Toppare L, Turker L, Yiğit S, Kısakürek D, Akbulut U. Eur Polym J 1990;26:255.
[15] Kısakürek D, Sen S, Aras L, Turker L, Toppare L. Polymer 1991; 32(7):1323.
[16] Kısakürek D, Yigit S. Eur Polym J 1991;27(9):955.
[17] Sen S, Kısakürek D. Polymer 1993;34(19):4146.
[18] Pulat M, Önal AM, Kısakürek D. New Polym Mater 1994;4(2):111.
[19] Aras L, Sen S, Kısakürek D. Polymer 1995;36(15):3013.
[20] Aydeniz K, Önal AM, Kısakürek D. Eur Polym J 2001;37:2017.
[21] Baecklund TG, Sandberg HGO, Oesterbacka R, Stubb H, Maekelae T, Jussila S. Synth Met 2005;148(1):87.
[22] Kinder L, Kanicki J, Petroff P. Synth Met 2004;146(2):181.
[23] Cirpan A, Ding L, Karasz FE. Polymer 2005;46(3):811.
[24] Thompson BC, Madrigal L, Pinto MR, Kang TS, Schanze KS, Reynolds JR. J Polym Sci, Part A: Polym Chem 2005;43(7):1417.
[25] Kiralp S, Toppare L, Yagci Y. Designed Monomers Polym 2004;7(1–2):3.
[26] Kiralp S, Toppare L, Yagci Y. Synth Met 2003;135–136:79.
[27] Yildiz HB, Kiralp S, Toppare L, Yilmaz F, Yagci Y, Ito K, et al. Polym Bull 2005;53(3):193.
[28] Arslan A, Kiralp S, Toppare L, Yagci Y. Int J Biol Macromol 2005; 35(3–4):163.
[29] Camurlu P, Cirpan A, Toppare L. J Electroanal Chem 2004;572(1):61.
[30] Camurlu P, Cirpan A, Toppare L. Synth Met 2004;146(1):91.
[31] Ak M, Cirpan A, Yilmaz F, Yagci Y, Toppare L. Eur Polym J 2005; 41(5):967.
[32] Argun AA, Cirpan A, Reynolds JR. Adv Mater (Weinheim, Germany) 2003;15(16):1338.
[33] Sonmez G, Wudl F. J Mater Chem 2005;15(1):20.
[34] Bulut U, Cirpan A. Synth Met 2005;148(1):65.
[35] Çakmak O, Baştürkmen M, Kısakürek D. Polymer 2004;45(16):5451.
[36] Baştürkmen M, Kısakürek D. J Macromol Sci, Pure Appl Chem 2004; A41(9):1071.
[37] Baştürkmen M, Kısakürek D. J Appl Polym Sci 2002;86(9):2232.
[38] Nicholson RS, Shain S. Anal Chem 1964;3:706.
[39] Boschke FL, Fresenenius W, Huber JFK, Pungur F, Rectinitz GA, Simon W, et al. Tables of spectrical data for structure determination of organic compounds, ^{13}C NMR, ^{1}H NMR, IR, MS, UV–vis. Berlin: Springer; 1983.